Geothermal Service
of Canada

Service géothermique
du Canada

THE ACOUSTIC PROPERTIES OF STRUCTURE I AND II
GAS HYDRATES BY BRILLOUIN SPECTROSCOPY

M. J. Clouter and H. Kiefte
Memorial University
St. John's, Newfoundland

Price/Prix: $7.75

Abstract

Measurements of the acoustic velocities in the Structure I methane and xenon hydrates and on Structure II tetrahydrofuran have been made for the first time. The results obtained using Brillouin spectroscopy are in reasonable agreement with earlier theoretical estimates for methane hydrate. Values average 0.88 of the ice velocity for methane hydrate, 0.76 for xenon hydrate and 0.97 for THF.

Résumé

Des mesures des vitesses acoustiques dans la Structure I (hydrates de méthane et de xénon) et dans la Structure II (tétrahydrofuranne) ont été réalisées pour la première fois. Les résultats obtenus par spectroscopie Brillouin concordent assez bien avec les estimations théoriques faites précédemment pour l'hydrate de méthane. Les valeurs moyennes sont de 0,88 de la vitesse dans la glace pour l'hydrate de méthane, 0,76 pour l'hydrate de xénon et de 0,97 pour le THF.

THE ACOUSTIC PROPERTIES OF

STRUCTURE I AND II GAS HYDRATES

BY BRILLOUIN SPECTROSCOPY

A report by

M. J. Clouter and H. Kiefte

Department of Physics

Memorial University of Newfoundland

St. John's, Newfoundland

Canada A1B 3X7

The purpose of this continuing project (as proposed March 16, 1981) is to investigate the properties of gas hydrates with emphasis being directed in particular to the determination of acoustic velocities in these materials. With respect to structure I hydrates, it was proposed (1) that efforts to improve the accuracy of longitudinal sound speed in methane hydrate be continued, and (2) that experiments be performed to measure the acoustic velocity in xenon hydrate. In addition, tetrahydrofuran (THF) hydrate was proposed as an example of the structure II case which was amenable to detailed acoustic velocity studies. These efforts have, for the most part, been successful; the exception being that measurements of shear wave velocities have, to date, been performed only in the case of THF hydrate.

The following report is written in two independent parts. Part A is devoted to the structure I hydrate results, and is a slightly modified version of a paper submitted to Geophysical Research Letters (Feb. 12/82) entitled "Determination of Acoustic Velocities in Xenon and Methane Hydrates by Brillouin Spectroscopy". Part B is concerned with the structure II (THF) hydrate results. Detailed descriptions of the apparatus have been presented in previous reports (Mar. 16, 1981; Apr. 15, 1980 and Dec. 8, 1979) and will not be repeated here.

PART A (Structure I hydrates)

Introduction

The presumed existence of extensive accumulations of natural gas hydrates in the ocean sediments, and particularly in the permafrost regions of Siberia (Chersky and Makogon 1970) and the North American Arctic (Bily and Dick 1974), has important economic and scientific

implications. Confirmation of the extent of these accumulations has, however, been hampered by a lack of knowledge regarding the properties of hydrates in general, and of methane hydrate in particular.

The presence of hydrate deposits has to a large extent been inferred from otherwise unexplained acoustic reflections which have been conditions appropriate for hydrate formation are believed to exist (Stoll et al. 1971; Stoll and Bryan 1979). The potential importance of seismic techniques in this connection is therefore clear. The effective application of such techniques is, however, contingent on an accurate knowledge of the acoustic velocities in these materials, and the extent to which they differ from ordinary ice. Such information (on pure hydrate samples) was not available prior to the theoretical estimates of Whalley (1980), and it is in this context that the first experimental determinations of acoustic velocities in pure methane and xenon hydrate are reported here.

The gas hydrates are crystalline, ice-like substances belonging to a class of inclusion compounds called clathrates, within which the ('guest') gas molecules are effectively trapped by the structure of the 'host' material (H_2O) (Davidson, 1973). Depending on the size of the guest molecule, two types of hydrates (denoted structures I and II) are possible. For methane and xenon it is the structure I lattice which forms. In this case the 46 water molecules comprising each 1.2 nm (cubic) unit cell form two dodecahedral and six tetrakaidecahedral cavities, or 'cages', such that when all cages are filled the empirical formula for methane hydrate, for example, is $CH_4 \cdot 5\frac{3}{4} H_2O$.

The dissociation pressure of methane hydrate at $0^O C$ is 380 psia (see Miller, 1973, for complete phase diagram). Although artifical samples have been obtained they were always opaque and not suitable

for light scattering work. Consequently, the development of a different technique was necessary in the present study. The investigation of xenon hydrate, with a much lower dissociation pressure of about 20 psia at $0^{O}C$, (Barrer and Edge, 1967) was helpful in this respect: while being of considerable interest in itself, it also served as a more experimentally tractable means of obtaining information about the most appropriate conditions for the formation of gas hydrates in general.

Brillouin spectroscopy is a relatively new experimental technique whose development has paralleled that of the laser and which has achieved a high level of technical sophistication. The technique involves the scattering of light by the ambient, thermally induced elastic waves in a transparent medium. The propagation velocity for a given wave is manifested as a Doppler shift in the frequency of the scattered radiation according to the Brillouin equation: $\nu_s = 2\nu_0(v/c)n \sin(\alpha/2)$. In this expression ν_0 and $\nu_0 \pm \nu_s$ are the frequencies of the incident and scattered light respectively, v is the phase velocity of the acoustic wave of frequency ν_s, c is the velocity of light in vacuum, n is the refractive index of the medium and α is the scattering angle. In the case of crystals there are, in general, three sets of symmetrical Brillouin doublets, one associated with longitudinal acoustic waves and two with transverse waves, whose frequency shifts (i.e. velocities) depend on crystal orientation. These shifts can be accurately measured by Fabry-Perot interferometry.

The principal advantage of the Brillouin scattering over the more conventional ultrasonic technique is that the elastic waves being probed are not artifically excited. Perturbation of the sample is consequently minimized and sample size can be greatly reduced (less than

1 mm^3). In addition, it is possible to probe small regions within a sample. The Brillouin scattering technique is therefore particularly suitable for the difficult-to-produce, high pressure samples in question, provided that samples with an acceptable degree of optical clarity can be obtained.

Apparatus and Sample Preparation

The Brillouin spectrometer used in these experiments has been described and shown schematically in other publications (see Gammon, et al., 1980). The incident light was provided by a single mode argon ion laser. The scattered light was spatially filtered and analysed at $\alpha = 90^{\circ}$ with a piezoelectrically scanned triple-pass Fabry-Perot interferometer, and detected by a cooled photomultiplier tube. The output from the photomultiplier was coupled to a data acquisition and stabilization system (Burleigh DAS 1). The multichannel analyser of the DAS system accumulated spectral data in the form of photon counts (intensity) versus channel number (proportional to the frequency of the scattered light).

The search for satisfactory methods of growing a suitable sample involved several changes in the sample cell, cryostat and gas handling system during the course of the work. Appropriate hydrate samples were eventually grown at the bottom of a 10 cm long quartz tube (1.5 mm I.D., 6.5 mm O.D.). A highly polished quartz plug was cemented into the bottom of the sample tube to provide for laser beam entry, while the top end of the quartz tube was flared and ground for pressure sealing to the gas handling system. Temperature control and cooling of the hydrate site was accomplished using a thermoelectric module. The entire cell assembly

and cooling module were enclosed in an evacuated plexiglass tube
(10 cm O.D.), the sample cell being suspended along its vertical axis. A
high pressure sealing unit and a gas inlet (and outlet) assembly permitted
gas flow to be directed to the sample site via a vertically adjustable
stainless steel (0.4 mm hypodermic) tube.

The gas handling system was constructed to permit, when desired,
a continuous flow of methane (or xenon) gas and water vapour through the
cell. After release from a pressure regulated (usually 800 psia) methane
storage bottle, the gas was filtered and passed through a metering valve,
through a high pressure water reservoir, into the cell via the hypodermic
tube whose bottom was adjusted to the desired height, and out of the system
through an adjustable relief valve and a simple flow meter. To permit
prefilling the system with methane (xenon) gas a back-fill connection was
provided for bypassing the water reservoir.

The initially chosen hydrate formation process consisted of
continuously flowing water-saturated methane through the hyprodermic tube
at about 800 psia and condensing it in the cold (-10°C to -20°C),
temperature-controlled region of the sample cell. The hypodermic tube
was adjusted vertically to keep its bottom end very close to the
growing hydrate surface at all times. Although hydrate samples were
obtained using this procedure, most of the formation occurred along the
cell walls and on the hypodermic tube. Gas flow over a column of single-
crystal ice, as well as over liquid water, was also investigated, but
in both cases a hydrate of poor optical quality was found to form
in the upper part of the sample region.

The best optical quality (but much smaller) methane hydrate samples were obtained by (1) growing a single crystal of ice to a height of about 5 mm from the bottom of the cell, (2) adjusting the cell temperature control such that the temperature of the top surface of the ice crystal was $0^{\circ}C$, and (3) pressurizing the system to 800 psia with methane gas via the back-fill valve. Under these conditions a cloudy layer of hydrate was found to form within a few hours and the (0.5 mm) sample was usually left, to allow continued growth for about one day. The conclusion that the samples were indeed hydrates was confirmed, first, by observing that they remained intact after the ice was melted immediately beneath them, and, second, by observing a profuse bubbling to occur when the system pressure was brought below the dissociation pressure.

The procedure adopted for xenon hydrate formation was identical, except that the backfilling pressure was only 45 psia. The xenon hydrate samples were of much higher optical quality than the methane hydrate samples, this was also borne out by the Brillouin spectra.

Light Scattering Results

After formation, the samples were cooled to $-10^{\circ}C$ to render them more resistant to melting or deterioration upon introduction of the laser beam. The incident laser light could be observed to pass through the ice as a narrow, clean, and well-focussed beam before encountering the hydrate layer. Very intense diffuse scattering occurred at this point, and it was obvious that the incident light was not penetrating into the hydrate layer to any significant depth in a spatially well-defined manner. Consequently it was necessary to spatially discriminate against the

intense parasitic scattering from the hydrate layer. This was accomplished by utilizing two 0.1 mm spatial filters in the optical detection system, and by extremely precise alignment and optimization of the scattering optics via observation of the Brillouin spectrum of ice just below the hydrate layer. A quartz refracting plate of 2 mm thickness was introduced in the axis of the scattering optics adjacent to cryostat so that, by slowly rotating it, the scattering volume being observed could be gradually adjusted upwards into the hydrate layer. It was only as a result of this procedure that xenon and hydrate spectra were observed and, in some cases, several days of continuous data acquisition were required.

Five independent xenon hydrate samples yielded a total of nine spectra exhibiting the longitudinal components of the hydrate and, in most cases, of ice as well. Only two spectra of methane hydrate exhibited Brillouin peaks of significant intensity, although five different methane hydrate samples were examined. The xenon hydrate/ice spectra were subject to a detailed investigation regarding their behavior versus height in the sample. It was found that a sharp reduction, and eventual disappearance of the ice signal occurred near the ice-hydrate discontinuity and this coincided with a maximum in the hydrate signal. Since there was also evidence that prolonged exposure to the laser beam caused local deterioration of the hydrate sample, this is probably the reason why the poorer optical quality methane hydrate samples yielded only two spectra.

With reference to Fig. 1 where the free spectral range (FSR) of the interferometer was 30.1 GHz, the frequency shift for xenon hydrate could be determined directly from the channel displacements by a simple calculation, $(\nu_s) = (FSR)(h' - R')/(R'' - R')$. However since the values

of interest are those relative to ice, it was considered more appropriate
to record the average difference in displacements between ice and the
hydrate signals. This corresponded to a (18.5 ± 1.5)% reduction in the
frequency shift (ν_{sh}) of xenon hydrate relative to ice (ν_{si}). The
uncertainty quoted here was determined from the scatter in all the data.
A particularly good xenon hydrate sample, that is one which was very clear
and produced by far the strongest spectra, yielded the greatest reduction
in frequency (20.0%). This would be expected for greater cage occupancy
(see Table I). Consequently it is assumed that much of the scatter in
the data arises from sample imperfections and slightly different cage
occupancies in the various samples.

The sound velocity (v_h) in xenon hydrate was also determined
relative to the velocity (v_i) in ice. Applying the Brillouin equation
to both substances, and then dividing one by the other yields:
$v_h/v_i = n_i \nu_{sh}/n_h \nu_{si}$. The index of refraction (n_h) of xenon hydrate was
calculated using the Lorentz-Lorenz relation $L\rho = (n^2 - 1)/(n^2 + 2)$
where ρ is the density. The Lorentz function L was determined for ice
using n = 1.312 ± 0.001 (International Critical Tables, 1926-33) and
$\rho = 0.9181 \pm 0.002$ g cm^{-3} at -10°C (Gammon et al., 1980 and Butkovich,
1959). The density of xenon hydrate was calculated from the lattice
constant measurements (1.197 nm) of von Stackelberg and Mueller (1954)
for the three cage occupancies of 75%, 90%, and 100%. The resulting
density values, indices of refraction and relative sound velocities
v_h/v_i, are shown on Table I.

The average reduction in frequency shift for methane hydrate
relative to ice was 9.4 ± 2%. Using the lattice constants (1.203 nm)

as noted by Davidson (1973) the relevant data for methane hydrate were calculated and are shown on Table I. Also included are the (absolute) longitudinal velocities of the methane and xenon hydrate based on the accurately measured average longitudinal velocity of ice 3830 m sec^{-1} at -10°C (Gammon, 1981). Uncertainty in these values is about ± 2%.

Discussion and Conclusions

To date, the only theoretical prediction of longitudinal velocities in hydrates has been carried out by Whalley (1980), who concluded that the value relative to ice was given by

$$(v_h/v_i)^2 = (\kappa_{Ti}/\kappa_{Th})(\rho_i/\rho_h)(1-\mu_h/1-\mu_i)(1+\mu_i/1+\mu_h)[(1-\alpha_i^2 TV_i/\kappa_{Ti}C_{pi})/$$
$$(1-\alpha_h^2 TV_h/\kappa_{Th}C_{ph})]$$

where κ_T is the isothermal compressibility, μ Poisson's ratio, T temperature, V molar volume, α volume thermal expansivity and C_p heat capacity. The velocity ratios were calculated (by the present authors) for various cage occupancies and are listed in Table I. The following data and assumptions were used (see Whalley, 1980): $\mu_i = \mu_h$, $\kappa_{Ti} = 12$ Mbar^{-1}, $\kappa_{Th}/\kappa_{Ti} = 1.135$, $\alpha_i = \alpha_h = 1.5 \times 10^{-4}$K^{-1}, $C_{pi} = 37.7$ J K^{-1} mol^{-1} and $\rho_i = 0.9181$ g cm^{-3}. The assumed heat capacity contribution from the guest molecules was $3R$ and $\frac{3}{2}R$ for translational and rotational motion respectively. Hydrate densities at the various cage occupancies and molar volumes were calculated from the lattice constants mentioned earlier. It should be noted that, because of the low mass of the methane molecules, the velocity results for methane hydrate (unlike xenon hydrate) are relatively independent of cage occupancy (see Table I).

It is expected that the temperature dependence of the velocities should correspond to that for ice, namely about -0.07%/$^{\circ}$C in the -20°C to 0°C range (Gammon, 1981).

In conclusion, measurements of the acoustic velocities in methane hydrate and xenon hydrate have been carried out for the first time. The values quoted depend on the assumed cage occupancy. This arises through the dependency of the index of refraction (in the Brillouin equation) on hydrate density. As based on a numerous experimental measurements (e.g. Galloway, et al., 1970) 90% cage occupancy is probably the most realistic value, and for this case the v_h value for methane hydrate at -10°C is about 3400 m/sec. This in turn corresponds to $v_h/v_i = 0.88$.

The present results are in reasonable agreement with the theoretical estimates of Whalley. It should perhaps be noted that the experimental values are preliminary. Further experiments for more accurate determinations, also of the transverse (shear) velocities, are in progress.

Table I. Acoustic velocities in Gas Hydrates (at -10°C)

	Cage Occupancy	Density g cm^{-3}	Index of Refraction	Experimental v_h/v_i	Theoretical v_h/v_i	Experimental v_h m sec^{-1}
Xenon hydrate	0.75	1.54	1.38	0.775	0.718	2970
	0.90	1.69	1.40	0.764	0.686	2930
	1.00	1.79	1.41	0.758	0.666	2900
Methane hydrate	0.75	0.882	1.33	0.894	0.956	3420
	0.90	0.900	1.34	0.887	0.946	3400
	1.00	0.912	1.35	0.880	0.940	3370

Part B (Structure II Hydrates)

Introduction

Because (liquid) THF and water are miscible in all proportions, and the mixtures can easily be solidified, it was decided to devote considerable time and effort towards growing a single crystal of THF hydrate. This was considered worthwhile since Brillouin scattering from a single crystal permits determination of the complete set of elastic constants for the material, and thus comprises the most detailed description of the elastic properties that it is possible to obtain. Given the elastic constants, the longitudinal and transverse velocities can be calculated for any crystalline direction, or appropriately averaged to represent the case of bulk, polycrystalline samples.

Apparatus and Sample Preparation

The cell used in this experiment is shown in figure 2. It was especially adapted for growing THF crystals from a cell previously used to study ice. The cell is made of 3 mm I.D. quartz tubing and is cooled thermoelectrically. A bronze split ring holder is used to thermally connect the cell. The THF hydrate was put in the quartz sample tube. The temperature was controlled by cooling from the bottom with the thermoelectric modules. This produced a thermal gradient of a few degrees from the diode to the fused quartz plug and was necessary to control the solid-liquid interface when growing a crystal. Dry nitrogen was circulated around the inside of the cell to keep moisture from condensing on the sample tube or on the inside face of the windows. Rotation of the sample, which was important in obtaining different orientations of a single crystal, was accomplished by rotating the top "Rotary Brass Holder".

The first attempts to grow a single crystal did not succeed. Laue photos showed many weak spots on the photos, characteristic of a polycrystalline samples, rather than the clear spots single crystals would have produced. As mentioned in a previous r ort, one of the problems encountered was tha' the seed crystal tended to detach itself from the bottom of the cell and would consequently melt after floating to the (warmer) top of the cell. It was also necessary to slightly increase the THF to H_2O volume ratio in the mixture from the theoretical (THF). 17 H_2O or 1.00 part THF to 3.77 parts H_2O by volume to prevent phase separation.

Several visually acceptably samples were produced and each was subsequently cooled to $0^\circ C$. X-ray Laue diffraction photographs were then obtained and the crystal orientations were determined using standard existing techniques in this laboratory. One of the samples proved to be a large (3 mm in diameter and 10 mm long) single crystal.

Light Scattering Results

Brillouin spectra were obtained at a series of 16 crystal orientations. The longitudinal and both transverse components were observed for a total of 43 independent measurements.

An index of refraction of 1.36 was caculated (via the Lorenz-Lorentz) relation and was utilized, together with the density value of 0.979 gm cm^{-3}, in analyzing the results. The elastic constants were consequently determined to be (in units of 10^8 N m^{-2}):

$$c_{11} = 143.6$$
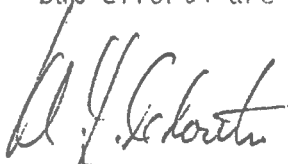$$c_{12} = 55.8$$
$$c_{44} = 31.8$$

These data in turn yielded a bulk modulus K = 85.08 and a shear modulus
G = 36.15 (both in units of 10^8 N m^{-2}). Appropriate averaging gives

$$\bar{V}_L = [(K + \frac{4}{3}G)/\rho]^{\frac{1}{2}} = 3690 \text{ m s}^{-1}$$

$$\bar{V}_T = (G/\rho)^{\frac{1}{2}} = 1922 \text{ m s}^{-1}$$

The respective ratios to the corresponding values for pure ice at 0°C are
then 0.97 and 0.99.

At least one other single crystal sample needs to be studied for
further confirmation of the above data.. This has not yet been accomplished,
but efforts are continuing.

M. J. Clouter

H. Kiefte

References

Barrer, R. M., and A. V. J. Edge, Gas hydrates containing argon, krypton and xenon: kinetics and energetics of formation and equilibria, Trans. Faraday Soc., 300, 1-24, 1967.

Bily, C., and J. W. L. Dick, Naturally occurring gas hydrates in the Mackenzie Delta, N.W.T., Bulletin of Canadian Petroleum Geology, 22, 340-353, 1974.

Butkovich, T. R., Thermal expansion of ice, Journal of Applied Physics, 30, 350-353, 1959.

Chersky, N., and Y. Makogon, Solid gas - World reserves are enormous, Oil Gas Invest., 10, 82, 1970.

Davidson, D. W., Clathrate hydrates, in Water: A Comprehensive Treatise, vol. 2, edited by F. Franks, pp. 115-234, Plenum Press, New York, 1973

Galloway, T. J., W. Ruska, P. S. Chappelear, and R. Kobayashi, Experimental measurement of hydrate numbers for methane and ethane and comparison with theoretical values, Ind. Eng. Chem. Fundam., 9, 237-243, 1970.

Gammon, P. H., H. Kiefte, and M. J. Clouter, Elastic constants of ice by Brillouin Spectroscopy, Journal of Glaciology, 25, 159-167, 1980.

Gammon, P. H., Brillouin spectroscopic studies of the elastic constants of artificial and natural ice samples, Ph.D. Thesis, Memorial University of Newfoundland, St. John's, Nfld., 1981.

International Critical Tables. 1926-1933. International Critical Tables. New York and London, McGraw-Hill Book Co., Inc.

Miller, S. L., The clathrate hydrates - Their nature and occurrence, in Physics and Chemistry of Ice, edited by E. Whalley, S. J. Jones, and L. W. Gold., pp. 42-50, Royal Society of Canada, Ottawa, 1973.

References Cont'd

Stackelberg, M. von, and H. R. Mueller, Solid gas hydrates, Part II,
Zeitschrift für Electrochemie, 58, 25-39, 1954.

Stoll, R. D., J. Ewing, and G. M. Bryan, Anomalous wave velocities in sediments
containing gas hydrates, Journal of Geophysical Research, 76, 2090-2094,
1971.

Stoll, R. D., and G. Bryan, Physical properties of sediments containing gas
hydrates, Journal of Geophysical Research, 84, 1629-1634, 1979.

Whalley, E., Speed of longitudinal sound in clathrate hydrates, Journal of
Geophysical Research, 85, 2539-2542, 1980.

Figure Caption

Fig. 1.

Reproduction of a Brillouin spectrum of xenon hydrate. The features
labelled R' and R" arise primarily from parasitic scattering at the incident
laser frequency for consecutive orders of Fabry-Perot transmission. The
features h' and h" are associated respectively with approaching and
receding longitudinal acoustic waves in xenon hydrate and the Doppler
shifts are 11.2 GHz. The sweep rate was programmed to increase the time
spent in the region of interest by a factor of 50. The spectrum represents
15 hrs of accumulation time at a laser power of 50 mw. The hydrate peaks
correspond to intensity levels of about 0.5 counts sec^{-1} with that of
the laser peaks about a million counts sec^{-1}.

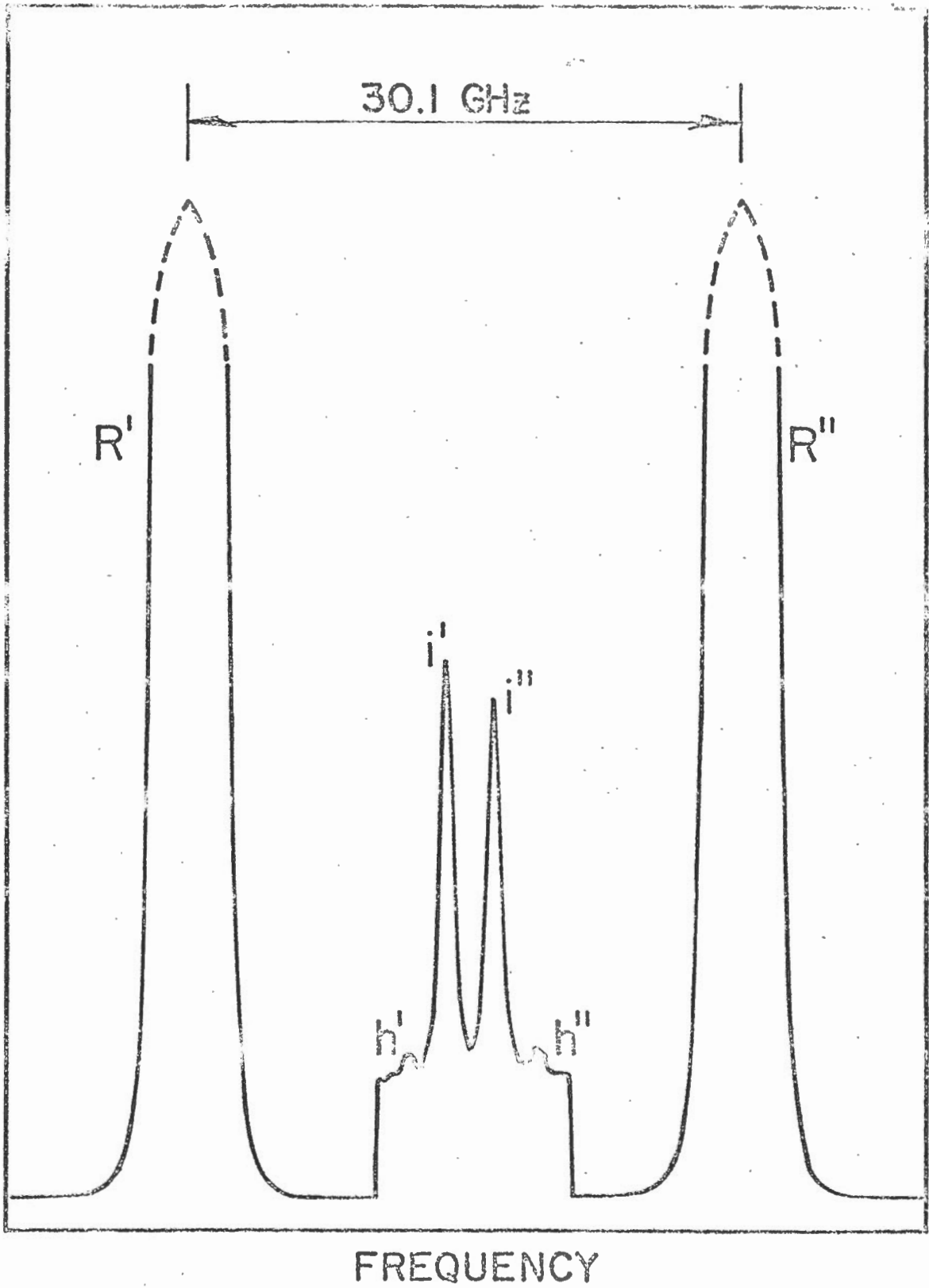Fig. 2.
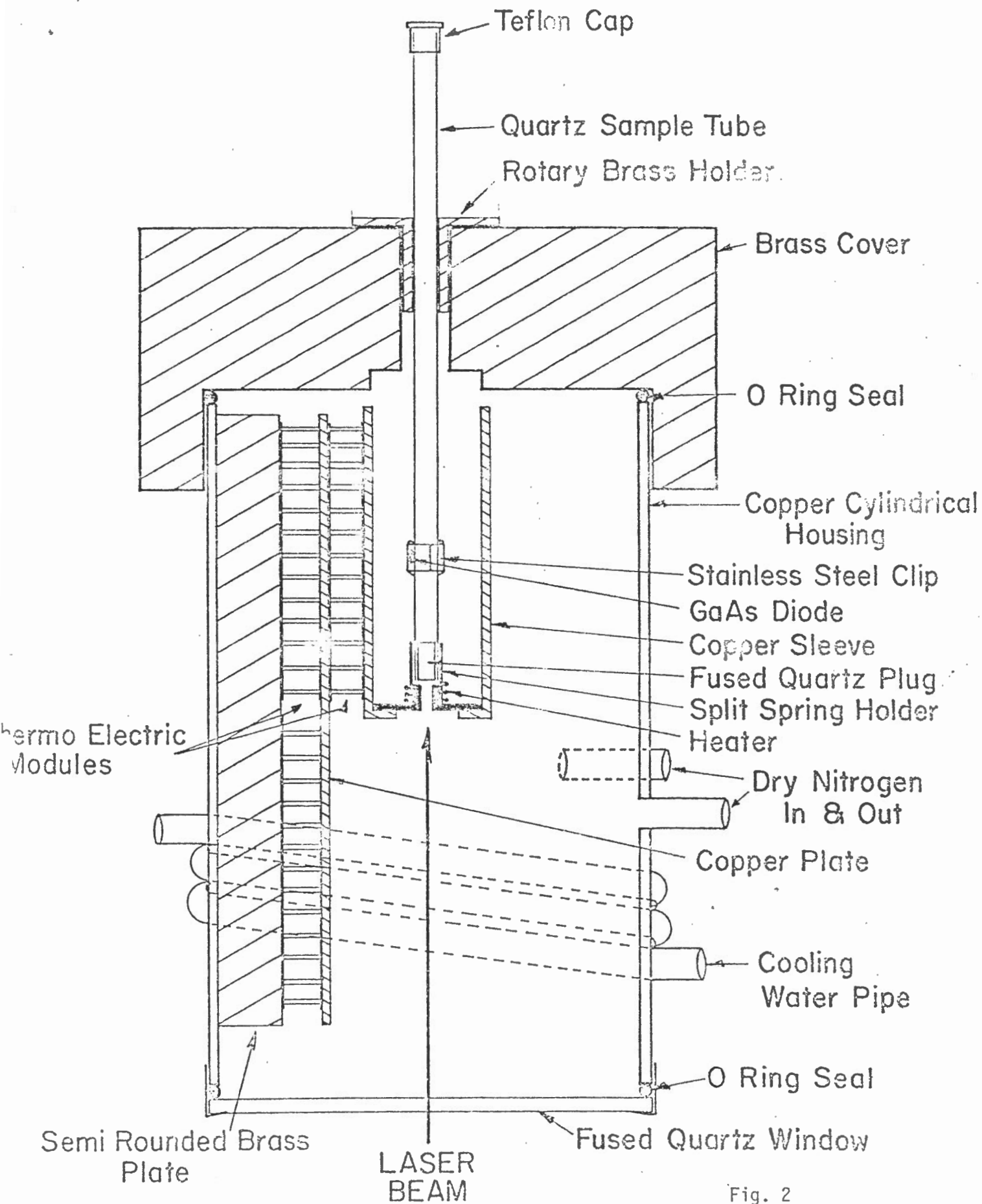
Cryostat and THF hydrate sample cell arrangement.

Fig. 1

Fig. 2